Title: E3 ubiquitin ligase WWP2 regulates stability of the chromatin remodeler ARID1B

Pradipta Hore[1,2], Sandipkumar Bambhaniya[1,2], Murali Dharan Bashyam[1†]

[1]Laboratory of Molecular Oncology, Centre for DNA Fingerprinting and Diagnostics, Hyderabad, Telangana, India;

[2]Graduate studies, Regional Centre for Biotechnology, Faridabad, India.

[†]**Address for correspondence:**

Murali Dharan Bashyam

Laboratory of Molecular Oncology, Centre for DNA Fingerprinting and Diagnostics, Uppal, Hyderabad 500039, India;

Phone: 91-40-27216112; Fax: 91-40-27216006;

Email: bashyam@cdfd.org.in; bashyam69@gmail.com

Abstract:

ARID1B, a key subunit of the SWI/SNF (also known as BAF) chromatin remodeling complex, is characterized as a canonical tumor suppressor across various cancer types. Although the downregulation of ARID1B transcript levels has been observed in many cancers, the regulation of ARID1B at the protein level is comparatively less studied. Here, we identify WWP2, an E3 ubiquitin ligase, as a novel interacting partner of ARID1B. We further show that using its WW domains, WWP2 interacts with the PPxY motif within the N-terminal intrinsically disordered region of ARID1B. The ability of wild-type (but not the catalytically inactive) WWP2 to modulate ARID1B protein stability was confirmed through cycloheximide chase assay. Interestingly, WWP2 appears to facilitate non-canonical K27- and K29-linked polyubiquitination of ARID1B, leading to the latter's proteasomal degradation. Additionally, silencing WWP2 expression results in a decrease in ubiquitination and a subsequent increase in ARID1B protein levels, indicating that WWP2 plays a crucial role in regulating ARID1B stability. Finally, based on several tumorigenic assays, we show that WWP2 may modulate ARID1B-mediated tumor suppression. Our results therefore highlight a novel mechanism of post-translational regulation of ARID1B, which may have implications in ARID1B-mediated tumor suppression.

Keywords:

SWI/SNF, ARID1B, WWP2, Ubiquitination, Proteasomal degradation, Tumor suppression.

Highlights:

- WWP2, an E3 ubiquitin ligase, is a novel interactor of ARID1B.
- WWP2 regulates ARID1B protein stability by K27- and K29-linked polyubiquitination mediated proteasomal degradation.
- WWP2 appears to modulate the tumor suppressor activity of ARID1B by controlling its abundance in tumor cells.

Introduction:

The mammalian SWItch/Sucrose Non-Fermentable (SWI/SNF) or BRG1/Brm associated factor (BAF) is a multi-subunit ATP-dependent chromatin remodeling complex involved in several cellular processes. The complex is categorised into three forms: canonical (cBAF), Polybromo (PBAF), and non-canonical (ncBAF) or GLTSCR1-like containing (GBAF)[1]. The AT-Rich Interaction Domain 1B (ARID1B) also called BAF250B, along with its paralog ARID1A, are mutually exclusive components of the cBAF complex [2]. ARID1B is a 250kDa protein containing multiple structural units including a 94-amino acid-long ARID domain, multiple LXXLL motifs that are expected to facilitate protein-protein interactions, a C-terminal Armadillo (ARM) repeat-containing BAF250_C domain that aids in BAF complex formation, and a nuclear localisation signal (NLS) (Supp fig. 1A)[3–5]. Majority of the protein is constituted by a classical intrinsically disordered region (IDR) (Supp fig. 1A**)** [6]. ARID1B has been reported to play important roles in fundamental cellular processes such as transcriptional regulation [7], mRNA splicing [8], DNA repair [9], and cell proliferation [10]. Multiple studies have revealed the regulation of *ARID1B* through mutations [11], chromosomal rearrangements [12], and epigenetic modifications such as promoter DNA methylation [13] with implications for tumorigenesis. However, the mechanism of ARID1B regulation at the protein level is largely unknown.

Ubiquitination is a common reversible post-translational protein modification majorly classified as mono or poly-ubiquitination [14]. Ubiquitin, a 76 amino acids long protein, uses either of seven lysine residues (K6, K11, K27, K29, K33, K48, and K63) or the α-amino group of the N-terminal methionine to effect linear or branched chain poly-ubiquitination with different combinations [15]. The ubiquitination process occurs in three steps: first, an ‘E1’ enzyme activates the ubiquitin molecule which is subsequently transferred to an ‘E2’ enzyme. The E2 interacts with the ubiquitin ligase ‘E3’ which in turn utilizes the C-terminal glycine of ubiquitin to link to the ε-amino group of a lysine residue on the substrate protein [16,17]. E3 ubiquitin ligases are categorized into three types according to their E2 binding domain structure and ubiquitin transfer mechanism: RING (Really Interesting Gene), HECT (homologous to the E6-associated protein carboxyl domain), and RBR (RING-between-RING) [18]. WW domain-containing E3 ubiquitin protein ligase 2 (WWP2), which belongs to the NEDD4 family of HECT ubiquitin ligases [19], is well characterized with respect to its role in transcription [20],

cell proliferation [19], and DNA repair [21]. WWP2 is a ~100 kDa protein that mainly comprises three domains: an N-terminal C2 domain, four WW domains responsible for the recognition of Proline-rich motifs on the substrates, and a C-terminal catalytic HECT domain responsible for the ubiquitin ligase activity [22]. *WWP2* is classified as an oncogene with well-established roles in hepatocellular [23,24], oral [25], breast [26], and prostate [26] carcinomas, as well as in glioma [27]. Previous studies have highlighted the involvement of WWP2 in regulating multiple cancer genes such as PTEN [19], OCT4 [20], etc.

Here, we report a novel interaction between ARID1B and WWP2. We further show that ARID1B stability could be regulated by WWP2 and that WWP2 can perhaps modulate ARID1B-mediated tumor suppression.

Material and methods:

Cell Culture and Modifications:

HEK293T (kind gift from Dr. Rashna Bhandari, Centre for DNA Fingerprinting and Diagnostics (CDFD), Hyderabad, India) and HCT116 cells (obtained from National Centre for Cell Science (NCCS), Pune, India) were cultured as described previously [5].

For generating knockdowns, ARID1B short hairpin RNAs (shRNA; Clone IDs TRCN0000420576 (sh2A) and TRCN0000107360 (sh3A)) and WWP2 shRNAs (5′-ATAAAGCGAAAGTAGGTGAGG-3′ (sh2); 5′-TTGACGATTATGCACCTTGGG-3′ (sh3)) were co-transfected with lentiviral packaging plasmids VSV.G and psPAX2 into HEK293T cells using polyethyleneimine (Sigma-Aldrich, St. Louis, MO, USA). Cell lysis was performed following previous protocol [5]. The extent of knockdown was determined by immunoblot analysis with specific antibodies. Tumorigenic assays including cell growth, viability (3-[4,5-dimethylthiazol-2-yl]-2,5 diphenyl tetrazolium bromide (MTT)), colony formation, and transwell migration assays were performed as described previously [5].

Antibodies and Immunoblotting:

Antibodies - WWP1 (Cat # ab43791) and ARID1B (Cat # ab57461) (Abcam, Cambridge, UK). Hemagglutinin (Cat # H6908), GAPDH (Cat # G8795), Myc clone 9E10 (Cat # M4439), Flag (Cat # F1804), and α-Tubulin (Cat # T6074) (Sigma-Aldrich, MO, USA). Halo (Cat # G9211) (Promega Corporations, Madison, WI, USA). ITCH (Cat # A8624), ARID1B (Cat # A15488)

(Abclonal, MA, USA). WWP2 (Cat # A302-936A) and all HRP-conjugated secondary antibodies (Thermo Fisher Scientific, Waltham, MA, USA). Near-infrared fluorophore-conjugated secondary antibodies (LI-COR Biosciences, Lincoln, NE, U.S.A). Immunoblotting was performed as described previously [5]. Following secondary antibody incubation, membranes were washed thrice with 1X TBST and imaged using either ChemiDoc (Cambridge Bioscience, Cambridge, United Kingdom) or a Li-Cor Odyssey CLx imaging system (LI-COR Biosciences).

Plasmids:

Full-length and C-terminal deletion constructs of ARID1B were used as described previously [5]. Wild-type and catalytically inactive mutants of WWP1 (C890S) and WWP2 (C838A), wild-type and lysine-mutated Ubiquitin constructs, and shRNA constructs for WWP2 were kind gifts from Dr. M. S. Reddy (CDFD, Hyderabad, India). Full length (Wild Type (WT)), as well as several domain deletions (C2 deletion (ΔC2), C2 plus all four WW domain deletions (ΔC2+ΔWW), and HECT domain deletion (ΔHECT) of WWP2 were generated. ARID1B PPxY deletion mutants were generated by site-directed mutagenesis using specific primers (PPxY #1 forward: 5' CCTCAGCAGCAGATGGGACAGCAAGGTGTG 3', reverse: 5' CACACCTTGCTGTCCCATCTGCTGCTGAGG 3'; PPxY #2 forward: 5' GGTAACTACTCCAGAAGTGGGGTGCCCAGT 3', reverse: 5' ACTGGGCACCCCACTTCTGGAGTAGTTACC 3'). All constructs were confirmed by sequencing.

Affinity purification and Mass spectrometry:

Liquid Chromatography Mass Spectrometry (LC-MS) (done twice - LMO1 and LMO2 (in duplicate)) was performed as per standard protocol. Briefly, HaloTag pull-down assay was carried out using the HaloTag Mammalian Pull-Down System (Promega Corporations) according to the manufacturer's protocol. 30 hours post transfection by Halo-vector or Halo-ARID1B, HEK293T cells were collected, washed, and lysed using Halo lysis buffer. Equilibrated HaloLink Resin was mixed with the lysate, incubated, washed, and eluted with SDS elution buffer. The eluted samples were analyzed by SDS-PAGE and detected by staining with Coomassie Brilliant Blue R250. The protein bands were excised from the gels and subjected to LC-MS (Taplin Biological Mass Spectrometry Facility, Harvard Medical School, Boston, MA 02115, USA). Interactors present in ARID1B interactome with >1.5-fold change in unique peptide numbers compared to vector control were selected for further analysis.

For SFB (Streptavidin-binding protein, Flag, and S-peptide) tagged proteins, Streptavidin-sepharose bead (Cat# 17-511301; GE Healthcare Bio-Science, Uppsala, Sweden) and for Halo tagged proteins, HaloTag bead (Halo pulldown and labeling kit, Cat# G6500; Promega Corporations) based affinity pulldown and antibody-based immunoprecipitations (Protein A Mag Sepharose, Cat # 28944006, Cytiva, United States) were performed as described previously [5,19].

Cycloheximide chase assay:

HEK293T cells were transfected with various combinations of plasmids and cycloheximide (Cat # 01810, Sigma-Aldrich, St. Louis, MO, USA) (50 µg/ml) was added 24 h post-transfection. Cells were harvested at the indicated time points and protein levels were determined by immunoblotting. Densitometry analysis of bands was done using Fiji software.

Ubiquitination assay:

HEK293T or HCT116 cells were transfected with different combinations of wild-type and mutant ubiquitin, each containing one wild-type lysine, along with SFB tagged ARID1B. At 24 h post-transfection, cells were treated with MG132 (Cat # C2211, Sigma-Aldrich) (10 µM) for 6 h. After harvesting, cells were denatured by 1% SDS followed by 10 min boiling at 95°C. The lysate was diluted with NETN lysis buffer (20 mM Tris-HCl pH 8.0, 100 mM NaCl, 1 mM EDTA, and 0.5% Nonidet P-40) to bring the SDS concentration to 0.1%. The solution was sonicated using the QSONICA Q500 (Qsonica L.L.C, Newtown, CT, USA) at 10% amplitude for 4 x 5s pulses and centrifuged at 14000 g for 10 min. The supernatant was added to pre-equilibrated streptavidin sepharose beads and incubated for 2 hours at 4°C. The analysis of ubiquitination was carried out by immunoblotting with anti-HA tag antibody.

Statistical analysis:

All data obtained from three independent experiments were represented as mean ±s.d. Student's t-test (unpaired) or two-way ANOVA test was used to determine the statistical significance of all experiments.

Results:

ARID1B interactome reveals possible involvement in multiple cellular processes

To understand the possible mechanism of ARID1B regulation at the post-translational level, we first examined its interactome using affinity purification of Halo-tagged ARID1B followed

by LC-MS in HEK293T cells (Fig 1A). We also mined an ARID1B interactome published earlier [8]. A combined robust analysis of all screens revealed a comprehensive list of 180 putative ARID1B interacting proteins (Supp Fig 1B, Supp Table 1). Gene ontology (GO) analysis revealed the ARID1B interactome to be enriched in fundamental cellular processes including G0 to G1 transition, nucleotide excision repair, and cytoplasmic translation (Fig 1B, 1C), in addition to previously identified roles in nucleosome binding, transcriptional regulation, and RNA splicing. Interestingly, scrutiny of the list of interacting proteins revealed only two E3 ubiquitin ligases, both belonging to the HECT family, namely WWP2 and its paralog WWP1 (Fig 1D).

ARID1B interacts with E3 ubiquitin ligases WWP1 and WWP2

To validate our affinity purification results, we tested the interaction of ARID1B with WWP1 and WWP2. We observed that ectopically expressed ARID1B interacted specifically with endogenous as well as ectopically expressed WWP1 and WWP2 in HEK293T (Fig. 2A and 2B). We further confirmed the existence of the ARID1B-WWP2 complex by demonstrating that WWP2 co-immunoprecipitated with endogenously expressed ARID1B in HCT116 cells (Fig. 2C). We generated multiple deletion constructs of SFB-tagged WWP2 (Fig. 2D) to map its ARID1B-binding region. Affinity precipitation results suggested that WW domains on WWP2 could be important for the interaction, as reported earlier [28] (Fig. 2E). Similarly, to map the binding site of WWP2 on ARID1B, we used a series of SFB-tagged ARID1B carboxy-terminal deletions generated previously [5] (Fig. 2F). We co-expressed each of these deletion constructs separately with full-length WWP2 or WWP1. The affinity purification results confirmed that both WWP2 (Fig. 2G) and WWP1 (Supp Fig 2) may interact with the N-terminal IDR region of ARID1B. We further verified this result by assessing the interaction with endogenous WWP2 (Fig. 2H).

The WW domain, typically 35–40 amino acids long, interacts with proline-rich motifs such as PPxY, PPLP, and phosphorylated serine/threonine-proline sites via its conserved tryptophan residues [29]. We detected 2 such PPxY motifs (PPxY#1 located at 523-526 aa, and PPxY#2 located at 785-788 aa) (Fig. 2F; Supp Fig. S1A) through ARID1B sequence analysis. We used site-directed mutagenesis to mutate these two sites in ARID1B and further evaluated their interaction with WWP2. Our results revealed a significant reduction of interaction between PPxY mutant ARID1B and WWP2 (Fig. 2H).

WWP2 regulates ARID1B protein level by ubiquitination-mediated degradation

To further characterize the functional significance of the interaction between ARID1B and WWP1/WWP2, we evaluated ARID1B levels in cells upon ectopic expression of WWP2. The presence of increasing amounts of wild-type (but not catalytically inactive mutant WWP2^{C838A}) WWP2 led to a reduction in ectopically expressed (Fig. 3A and 3B) and endogenous (Fig. 3C) ARID1B levels. Similar results were obtained with wild-type and catalytically inactive mutant WWP1^{C890S} (Supp Fig 3A). On the other hand, we observed an elevation in endogenous ARID1B protein levels upon shRNA-mediated stable knockdown of WWP2 (Fig. 3D). Further, cycloheximide chase experiments revealed that the downregulation of WWP2 caused a significant increase in the stability of ectopically expressed ARID1B (Fig. 3E and 3F). Similarly, we observed a significant reduction in ARID1B half-life in the presence of WT but not the catalytic mutant form of WWP2 (Fig. 3G and 3H) or WWP1 (Supp Fig 3B and 3C). Given that WWP2 is a known HECT-domain-containing E3 ligase involved in the ubiquitin-mediated proteasomal degradation of its substrates, it is expected to regulate ARID1B levels in a similar manner. Indeed, treatment with the proteasome inhibitor MG132 caused a significant elevation in ARID1B protein levels in HCT116 cells overexpressing wild-type WWP2, whereas no such increase was observed in cells expressing the catalytic mutant WWP2 or the vector control (Fig. 3I). Further, in the presence of MG132, ARID1B ubiquitination levels were readily elevated by wild-type but not catalytically inactive WWP2 (Fig. 3J). This result was further supported by a reduction in the levels of ARID1B ubiquitination upon WWP2 knockdown in HEK293T (Fig. 3K) as well as HCT116 cells (Fig. 3L). Interestingly, a ubiquitination assay using various ubiquitin mutants revealed that WWP2 appeared to facilitate K27 and K29-linked polyubiquitin chain formation on ARID1B (Fig. 3M).

WWP2 potentiates ARID1B depletion-dependent tumorigenic features

Having established a critical role of WWP2 in regulating ARID1B protein levels, and given the previously established oncogenic and tumor suppressor functions of WWP2 and ARID1B, respectively, we attempted to explore the role of WWP2 in ARID1B downregulation-dependent tumor progression. To this end, we first generated ARID1B knockdown in HCT116 cells and validated its tumor suppressor function using various assays; there was a significant elevation in several tumorigenic features due to a reduction in ARID1B levels (Supp Fig 4A-D), as previously reported [10,13]. We subsequently generated WWP2 knockdown in HCT116 cells already possessing knockdown of ARID1B, which caused a reduction in the elevated tumorigenic phenotypes resulting from ARID1B knockdown (Fig. 4A-F).

Discussion:

In the current study, we attempted to determine modes of regulation of ARID1B, an important chromatin remodeler, at the protein level. The scrutiny of ARID1B-interactome, generated in-house and elsewhere, revealed HECT family ubiquitin ligases WWP1 and WWP2 as novel interactors of ARID1B. Our results revealed ARID1B N-terminal PPxY motifs spanning amino acids 437-1035 located within the IDR to be involved in interaction with WWP1/WWP2 suggesting a complete non-overlap with the ARID1B region (C-terminal BAF_250C domain) responsible to form the BAF complex [4]. Interestingly, mutating both PPxY motifs within this region reduced but did not entirely disrupt ARID1B's interaction with WWP1/P2, suggesting that additional proline-rich motifs in ARID1B could contribute to binding with the WW domains of WWP1/WWP2.

Previous reports showed that E3 ubiquitin ligases WWP1 and WWP2 shared multiple common substrates like PTEN [19,30], Dvl2 [31,32], and Atophin-1 [33]. Our results indicate ARID1B to be yet another common substrate for these two E3 ligases. WWP1 and WWP2 have been shown to form heterodimers and regulate cellular homeostasis of p73 and ΔNp73 [34]. While we confirmed the independent binding of WWP1 and WWP2 to ARID1B; further investigation is needed to determine whether this interaction is competitive, cooperative or independent of each other. Interestingly, WWP2 is known to regulate another SWI/SNF complex component, Srg3 (mouse homolog of human BAF155/SMARCC1) [35]. Further, WWP2 is shown to utilize different ubiquitination chains including K11, K27, K48, and K63, to perform poly-ubiquitination [36]. Of note, K63-linked ubiquitination of Dvl2 by WWP2 was shown to be required for the former's ability to form condensates [31]. It will be interesting to determine if the ubiquitination of ARID1B has any effect on its phase separation properties [6]. Previously, ARID1B has been reported to be part of ubiquitin ligase system containing Cul2, Elo C and Roc1 responsible for histone H2B monoubiquitination . Mutation in BC box motif in ARID1B results in auto-ubiquitination followed by proteasomal degradation by the same complex [37].

Among the various Lysine residues that participate in polyubiquitination, K48- and K63-linked polyubiquitination are the most extensively studied. K48-linked polyubiquitination is primarily associated with proteasomal degradation, whereas K63-linked polyubiquitination is non-degradative and predominantly involved in mediating protein interactions and activating signaling pathways [15,38]. Recent research has highlighted the role of K11- and K27-linked polyubiquitination in ubiquitin-mediated proteasomal degradation [39–41]. In this study, we

demonstrated that WWP2 mediates K27 and K29-linked polyubiquitination of ARID1B, resulting in its proteasomal degradation. In other studies, WWP2 has been reported to form a complex with another HECT E3 ubiquitin ligase, ITCH, to mediate the K27-linked non-canonical poly-ubiquitination of the SHP-1 phosphatase [42]. Interestingly, ITCH was identified in only one of our ARID1B interactomes (LMO1) but could not be independently validated using pull down-immunoblotting (Supp Fig 5). Recent studies showed that K27-linked ubiquitination is majorly a nuclear modification and plays an important part in cell proliferation, DNA repair, and cell cycle progression [43] [38]. Further studies are required to find any relation of ARID1B K27-ubiquitination with these processes. K29-linked polyubiquitination has also been associated with regulation of protein levels [44].

ARID1B has been extensively studied for its critical role in tumor suppression presumably due to its role in transcriptional activation of classical tumor suppressors including CDKN1A (p21), CDKN1B (p27), and TP53 [5,45] and ARID1B downregulation has been linked to oncogenic stimulation [10,13]. Here, we demonstrated that the oncogenic properties associated with ARID1B downregulation can be potentially reversed by concomitant downregulation of WWP2. This discovery is important in the context of recent reports highlighting the utility of targeting synthetic lethal genes linked to BAF complex components in several cancers [46,47]. WWP2 could thus potentially represent a promising therapeutic target for addressing ARID1B-mediated tumorigenesis. To summarise, this study reveals a novel mechanism of non-canonical polyubiquitination-mediated post-translational regulation of ARID1B by the ubiquitin ligase WWP2. WWP2 upregulation decreases ARID1B protein levels, promoting tumorigenic phenotypes.

Author Contributions:

PH: Conceptualization, Methodology, Investigation, Formal analysis, Validation, Data Curation, Visualization, Writing- Original draft, Writing - Review & Editing. **SB:** Methodology, Investigation, Formal analysis, Validation, Visualization, Writing - Review & Editing. **MDB:** Conceptualization, Resources, Formal analysis, Supervision, Project administration, Funding acquisition, Writing- Original draft, Writing - Review & Editing.

Acknowledgements:

We thank Dr. M. S. Reddy, Centre for DNA Fingerprinting and Diagnostics (CDFD), Hyderabad, India, for providing wild-type and catalytically inactive mutants of WWP1 and

WWP2, wild-type and lysine-mutated Ubiquitin constructs, and shRNA constructs for WWP2. HEK293T cells were kind gift from Dr. Rashna Bhandari, Centre for DNA Fingerprinting and Diagnostics (CDFD), Hyderabad, India. We thank Animireddy Srinivas for initial ARID1B interacome data generation.

Funding:

The work was supported by a grant (BT/PR13948/BRB/10/1406/2015) from the Department of Biotechnology, Ministry of Science and Technology, India, to MDB. PH and SB, registered PhD students of the Regional Centre for Biotechnology, Faridabad, India, acknowledge the Department of Biotechnology, Government of India, for Junior and Senior Research Fellowships.

Conflict of Interest:

All authors declare no conflict of interest.

References:

[1] Mashtalir N, D'Avino AR, Michel BC, Luo J, Pan J, Otto JE, et al. Modular Organization and Assembly of SWI/SNF Family Chromatin Remodeling Complexes. Cell 2018;175:1272-1288.e20. https://doi.org/10.1016/j.cell.2018.09.032.

[2] Wu JN, Roberts CWM. ARID1A Mutations in Cancer: Another Epigenetic Tumor Suppressor? Cancer Discov 2013;3:35–43. https://doi.org/10.1158/2159-8290.CD-12-0361.

[3] Wilsker D, Patsialou A, Zumbrun SD, Kim S, Chen Y, Dallas PB, et al. The DNA-binding properties of the ARID-containing subunits of yeast and mammalian SWI/SNF complexes. Nucleic Acids Res 2004;32:1345–53. https://doi.org/10.1093/nar/gkh277.

[4] Sandhya S, Maulik A, Giri M, Singh M. Domain architecture of BAF250a reveals the ARID and ARM-repeat domains with implication in function and assembly of the BAF remodeling complex. PLoS One 2018;13:1–26. https://doi.org/10.1371/journal.pone.0205267.

[5] Animireddy S, Kavadipula P, Kotapalli V, Gowrishankar S, Rao S, Bashyam MD. Aberrant cytoplasmic localization of ARID1B activates ERK signaling and promotes oncogenesis. J Cell Sci 2021;134:jcs251637. https://doi.org/10.1242/jcs.251637.

[6] Patil A, Strom AR, Paulo JA, Collings CK, Ruff KM, Shinn MK, et al. A disordered region controls cBAF activity via condensation and partner recruitment. Cell 2023;186:4936-4955.e26. https://doi.org/10.1016/j.cell.2023.08.032.

[7] Azad P, Caldwell AB, Ramachandran S, Spann NJ, Akbari A, Villafuerte FC, et al. ARID1B, a molecular suppressor of erythropoiesis, is essential for the prevention of Monge's disease. Exp Mol Med 2022;54:777–87. https://doi.org/10.1038/s12276-022-00769-1.

[8] Reddy D, Bhattacharya S, Levy M, Zhang Y, Gogol M, Li H, et al. Paraspeckles interact with SWI/SNF subunit ARID1B to regulate transcription and splicing. EMBO Rep 2023;24:e55345. https://doi.org/https://doi.org/10.15252/embr.202255345.

[9] Watanabe R, Ui A, Kanno SI, Ogiwara H, Nagase T, Kohno T, et al. SWI/SNF factors required for cellular resistance to dna damage include arid1a and arid1b and show interdependent protein stability. Cancer Res 2014;74:2465–75. https://doi.org/10.1158/0008-5472.CAN-13-3608.

[10] Deogharkar A, Singh SV, Bharambe HS, Paul R, Moiyadi A, Goel A, et al. Downregulation of ARID1B, a tumor suppressor in the WNT subgroup medulloblastoma, activates multiple oncogenic signaling pathways. Hum Mol Genet 2021;30:1721–33. https://doi.org/10.1093/hmg/ddab134.

[11] Wang Z, Chen K, Jia Y, Chuang J-C, Sun X, Lin Y-H, et al. Dual ARID1A/ARID1B loss leads to rapid carcinogenesis and disruptive redistribution of BAF complexes. Nat Cancer 2020;1:909–22. https://doi.org/10.1038/s43018-020-00109-0.

[12] Sausen M, Leary RJ, Jones S, Wu J, Reynolds CP, Liu X, et al. Integrated genomic analyses identify ARID1A and ARID1B alterations in the childhood cancer neuroblastoma. Nat Genet 2013;45:12–7. https://doi.org/10.1038/ng.2493.

[13] Khursheed M, Kolla JN, Kotapalli V, Gupta N, Gowrishankar S, Uppin SG, et al. ARID1B, a member of the human SWI/SNF chromatin remodeling complex, exhibits tumour-suppressor activities in pancreatic cancer cell lines. Br J Cancer 2013;108:2056–62. https://doi.org/10.1038/bjc.2013.200.

[14] Swatek KN, Komander D. Ubiquitin modifications. Cell Res 2016;26:399–422. https://doi.org/10.1038/cr.2016.39.

[15] Davis ME, Gack MU. Ubiquitination in the antiviral immune response. Virology 2015;479–480:52–65. https://doi.org/https://doi.org/10.1016/j.virol.2015.02.033.

[16] Behera A, Reddy ABM. WWP1 E3 ligase at the crossroads of health and disease. Cell Death Dis 2023;14:853. https://doi.org/10.1038/s41419-023-06380-0.

[17] Damgaard RB. The ubiquitin system: from cell signalling to disease biology and new therapeutic opportunities. Cell Death Differ 2021;28:423–6. https://doi.org/10.1038/s41418-020-00703-w.

[18] Buetow L, Huang DT. Structural insights into the catalysis and regulation of E3 ubiquitin ligases. Nat Rev Mol Cell Biol 2016;17:626–42. https://doi.org/10.1038/nrm.2016.91.

[19] Maddika S, Kavela S, Rani N, Palicharla VR, Pokorny JL, Sarkaria JN, et al. WWP2 is an E3 ubiquitin ligase for PTEN. Nat Cell Biol 2011;13:728–33. https://doi.org/10.1038/ncb2240.

[20] Xu H, Wang W, Li C, Yu H, Yang A, Wang B, et al. WWP2 promotes degradation of transcription factor OCT4 in human embryonic stem cells. Cell Res 2009;19:561–73. https://doi.org/10.1038/cr.2009.31.

[21] Caron P, Pankotai T, Wiegant WW, Tollenaere MAX, Furst A, Bonhomme C, et al. WWP2 ubiquitylates RNA polymerase II for DNA-PK-dependent transcription arrest and repair at DNA breaks. Genes Dev 2019;33:684–704. https://doi.org/10.1101/gad.321943.118.

[22] Jiang H, Chiang CY, Chen Z, Nathan S, D'Agostino G, Paulo JA, et al. Enzymatic analysis of WWP2 E3 ubiquitin ligase using protein microarrays identifies autophagy-related substrates. J Biol Chem 2022;298. https://doi.org/10.1016/j.jbc.2022.101854.

[23] Qin Y, Xu S-Q, Pan D-B, Ye G-X, Wu C-J, Wang S, et al. Silencing of WWP2 inhibits adhesion, invasion, and migration in liver cancer cells. Tumour Biol J Int Soc Oncodevelopmental Biol Med 2016;37:6787–99. https://doi.org/10.1007/s13277-015-4547-z.

[24] Xu S-Q, Qin Y, Pan D-B, Ye G-X, Wu C-J, Wang S, et al. Inhibition of WWP2 suppresses proliferation, and induces G1 cell cycle arrest and apoptosis in liver cancer cells. Mol Med Rep 2016;13:2261–6. https://doi.org/10.3892/mmr.2016.4771.

[25] Fukumoto C, Nakashima D, Kasamatsu A, Unozawa M, Shida-Sakazume T, Higo M, et al. WWP2 is overexpressed in human oral cancer, determining tumor size and poor prognosis in patients: downregulation of WWP2 inhibits the AKT signaling and tumor growth in mice. Oncoscience 2014;1:807–20. https://doi.org/10.18632/oncoscience.101.

[26] Soond SM, Smith PG, Wahl L, Swingler TE, Clark IM, Hemmings AM, et al. Novel WWP2 ubiquitin ligase isoforms as potential prognostic markers and molecular targets in cancer. Biochim Biophys Acta - Mol Basis Dis 2013;1832:2127–35. https://doi.org/https://doi.org/10.1016/j.bbadis.2013.08.001.

[27] Liang J, Qi W-F, Xie S, Wang W-F, Zhang X-L, Zhou X-P, et al. Expression of WW domain-containing protein 2 is correlated with pathological grade and recurrence of glioma. J Cancer Res Ther 2017;13:1032–7. https://doi.org/10.4103/0973-1482.176176.

[28] Jiang J, Wang N, Jiang Y, Tan H, Zheng J, Chen G, et al. Characterization of substrate binding of the WW domains in human WWP2 protein. FEBS Lett 2015;589:1935–42. https://doi.org/https://doi.org/10.1016/j.febslet.2015.05.021.

[29] Ingham RJ, Colwill K, Howard C, Dettwiler S, Lim CSH, Yu J, et al. WW domains provide a platform for the assembly of multiprotein networks. Mol Cell Biol 2005;25:7092–106. https://doi.org/10.1128/MCB.25.16.7092-7106.2005.

[30] Lee Y-R, Chen M, Lee JD, Zhang J, Lin S-Y, Fu T-M, et al. Reactivation of PTEN tumor suppressor for cancer treatment through inhibition of a MYC-WWP1 inhibitory pathway. Science 2019;364. https://doi.org/10.1126/science.aau0159.

[31] Vamadevan V, Chaudhary N, Maddika S. Ubiquitin-assisted phase separation of dishevelled-2 promotes Wnt signalling. J Cell Sci 2022;135:jcs260284. https://doi.org/10.1242/jcs.260284.

[32] Zhao D, Zhong G, Li J, Pan J, Zhao Y, Song H, et al. Targeting E3 Ubiquitin Ligase WWP1 Prevents Cardiac Hypertrophy Through Destabilizing DVL2 via Inhibition of K27-Linked Ubiquitination. Circulation 2021;144:694–711. https://doi.org/10.1161/CIRCULATIONAHA.121.054827.

[33] Wood JD, Yuan J, Margolis RL, Colomer V, Duan K, Kushi J, et al. Atrophin-1, the

DRPLA gene product, interacts with two families of WW domain-containing proteins. Mol Cell Neurosci 1998;11:149–60. https://doi.org/10.1006/mcne.1998.0677.

[34] Chaudhary N, Maddika S. WWP2-WWP1 ubiquitin ligase complex coordinated by PPM1G maintains the balance between cellular p73 and ΔNp73 levels. Mol Cell Biol 2014;34:3754–64. https://doi.org/10.1128/MCB.00101-14.

[35] Luo X, Wang B, Tang F, Zhang J, Zhao Y, Li H, et al. Wwp2 targets SRG3, a scaffold protein of the SWI/SNF-like BAF complex, for ubiquitination and degradation. Biochem Biophys Res Commun 2014;443:1048–53. https://doi.org/10.1016/j.bbrc.2013.12.089.

[36] You S, Xu J, Guo Y, Guo X, Zhang Y, Zhang N, et al. E3 ubiquitin ligase WWP2 as a promising therapeutic target for diverse human diseases. Mol Aspects Med 2024;96:101257. https://doi.org/https://doi.org/10.1016/j.mam.2024.101257.

[37] Li XS, Patrick T, Tatsushi M, Jessica E. T, and Tanese N. Mammalian SWI/SNF-A Subunit BAF250/ARID1 Is an E3 Ubiquitin Ligase That Targets Histone H2B. Mol Cell Biol 2010;30:1673–88. https://doi.org/10.1128/MCB.00540-09.

[38] Yau R, Rape M. The increasing complexity of the ubiquitin code. Nat Cell Biol 2016;18:579–86. https://doi.org/10.1038/ncb3358.

[39] Matsumoto ML, Wickliffe KE, Dong KC, Yu C, Bosanac I, Bustos D, et al. K11-linked polyubiquitination in cell cycle control revealed by a K11 linkage-specific antibody. Mol Cell 2010;39:477–84. https://doi.org/10.1016/j.molcel.2010.07.001.

[40] Zhou Q, Zhang J. K27-linked noncanonic ubiquitination in immune regulation. J Leukoc Biol 2022;111:223–35. https://doi.org/https://doi.org/10.1002/JLB.4RU0620-397RR.

[41] Locke M, Toth JI, Petroski MD. Lys11- and Lys48-linked ubiquitin chains interact with p97 during endoplasmic-reticulum-associated degradation. Biochem J 2014;459:205–16. https://doi.org/10.1042/BJ20120662.

[42] Aki D, Li H, Zhang W, Zheng M, Elly C, Lee JH, et al. The E3 ligases Itch and WWP2 cooperate to limit T(H)2 differentiation by enhancing signaling through the TCR. Nat Immunol 2018;19:766–75. https://doi.org/10.1038/s41590-018-0137-8.

[43] Shearer RF, Typas D, Coscia F, Schovsbo S, Kruse T, Mund A, et al. K27-linked

ubiquitylation promotes p97 substrate processing and is essential for cell proliferation. EMBO J 2022;41:e110145. https://doi.org/10.15252/embj.2021110145.

[44] Liu C, Liu W, Ye Y, Li W. Ufd2p synthesizes branched ubiquitin chains to promote the degradation of substrates modified with atypical chains. Nat Commun 2017;8:14274. https://doi.org/10.1038/ncomms14274.

[45] Inoue H, Giannakopoulos S, Parkhurst CN, Matsumura T, Kono EA, Furukawa T, et al. Target genes of the largest human SWI/SNF complex subunit control cell growth. Biochem J 2011;434:83–92. https://doi.org/10.1042/BJ20101358.

[46] Wanior M, Krämer A, Knapp S, Joerger AC. Exploiting vulnerabilities of SWI/SNF chromatin remodelling complexes for cancer therapy. Oncogene 2021;40:3637–54. https://doi.org/10.1038/s41388-021-01781-x.

[47] Helming KC, Wang X, Wilson BG, Vazquez F, Haswell JR, Manchester HE, et al. ARID1B is a specific vulnerability in ARID1A-mutant cancers. Nat Med 2014;20:251–4. https://doi.org/10.1038/nm.3480.

Fig.1: The ARID1B interactome reveals its involvement in multiple cellular processes. Schematic representation of methodology to determine the ARID1B interactome (A). Gene Ontology (GO) analysis of the ARID1B interactome for 'cellular processes' (B) and 'molecular function' (C). Ubiquitin ligases interacting with ARID1B identified from multiple interactome lists (D).

Fig. 2: WWP1 and WWP2 are novel interacting partners of ARID1B. Affinity-based pull-down to validate the interaction of Halo-tagged ARID1B with endogenous (A) and ectopically expressed (B) WWP1 and WWP2 in HEK293T cells. * indicates non-specific band. Immunoprecipitation of endogenous ARID1B validating the interaction with WWP2 in HCT116 cells (C). Schematic representation of the full-length and various deletion mutants of WWP2 (D) and assessment of their interaction with ARID1B (E). Schematic representation of the full-length and various C-terminal deletion mutants highlighting the location of PPxY motifs in ARID1B (F) and assessment of their interactions with ectopically expressed (G) and endogenous (H) WWP2. Interaction between endogenous WWP2 and wild-type or various PPxY mutated derivatives of ARID1B (I).

Fig. 3: ARID1B is subjected to WWP2-mediated degradation via K27/K29-linked ubiquitination. Assessment of ectopically expressed ARID1B levels when exposed to increasing amounts of wild-type (left) or catalytically inactive mutant (right) of WWP2 in HEK293T cells (A); quantification of change in ARID1B protein levels is shown in panel B. Change in endogenous ARID1B protein levels under similar condition as (A) is shown in panel (C). Evaluation of ARID1B protein levels upon shRNA-mediated knockdown of WWP2 in HEK293T (D). Protein intensity fold change is represented as mean ± SD. Assessment of endogenous ARID1B levels by cycloheximide chase assay upon shRNA-mediated down-regulation of WWP2 (E); quantitation of change in ARID1B levels is shown in panel F. Evaluation of ARID1B protein stability by cycloheximide chase assay in the presence or absence of wild-type or mutant WWP2 (G); quantitation of change in ARID1B levels is shown in panel H. Evaluation of change in ARID1B protein levels in the presence of wild-type or mutant WWP2 upon MG132 treatment in HEK293T cells (I). Evaluation of ARID1B ubiquitination in the presence of ectopically expressed wild-type or mutant WWP2 in HEK293T cells (J) or upon shRNA-mediated knockdown of WWP2 in HEK293T (K) and HCT116 (L) cells. Assessment of specific poly-ubiquitin chain formation of ARID1B in the presence of wild-type WWP2 (M). All quantitation (panels B, F and H) are from three

independent experiments. EV, empty vector; WT, wildtype; MT, mutant; UT, un-transfected. *P<0.05; **P<0.01; ***P<0.001; ****P<0.0001.

Fig. 4: WWP2 modulates ARID1B tumor suppressor properties. shRNA mediated knockdown of ARID1B and WWP2 in HCT116 colorectal cancer cells (A). Colony formation (B, C), Transwell migration (D, E), and Cell growth (F, G) assays were performed with various combinations of down regulation of ARID1B and WWP2, as indicated. All results from three experiments are presented as mean ± SD. *P<0.05; **P<0.01; ****P<0.0001; ns, not significant

Fig. 5: Graphical Abstract. The ubiquitin ligase WWP2 causes polyubiquitination and subsequent proteasomal degradation of ARID1B (top). Low WWP2 levels maintain normal ARID1B levels (bottom left). Increased WWP2 levels result in reduced ARID1B that may potentiate tumorigenic features.

Supp. Fig. 1: (related to Fig. 1): Schematic representation of ARID1B domains (A). Common interacting proteins identified in multiple ARID1B interactome screens.

Supp. Fig. 2: (related to Fig. 2): Interaction between Myc-WWP1 and full-length and various C-terminal deletion mutants of SFB-tagged ARID1B (B).

Supp. Fig. 3: (related to Fig. 3): Assessment of endogenous ARID1B levels when exposed to increasing amounts of ectopically expressed wild-type or mutant WWP1 (A). Evaluation of ARID1B protein stability by cycloheximide chase assay in the presence or absence of wild-type or mutant WWP1 (B); quantification is shown in panel C. WT, wildtype; MT, mutant; UT, untransfected. Quantifications (panel C) are from three independent experiments. *P<0.05; **P<0.01; ****P<0.0001

Supp. Fig. 4: (related to Fig. 4): Cell growth (A), viability (B), and colony formation (C, D) assays performed in HCT116 cells following ARID1B knockdown. All quantitation (panels A, B and C) are from three independent experiments. *P<0.05; **P<0.01; ****P<0.001; ****P<0.0001

Supp. Fig. 5: Absence of complex formation between ARID1B and ITCH.

Supp Table 1: List of common interacting partners of ARID1B obtained from different interactomes

SMARCD3	PRPF19	C1QBP	ABCD3	TUBG1	HAX1
STT3A	RPL12	DNAJC11	HNRNPH1	COQ8A	NUP205
BYSL	CDIPT	PCBP1	PGAM5	TIMMDC1	TOMM40
PFKP	TUBB	TCP1	CHCHD3	SLC25A6	SMARCA2
IRS4	SMARCB1	VIM	HNRNPD	TMCO1	TIMM17B
SLC25A3	ERLIN2	TMEM209	SS18	KHSRP	SNRNP200
RPS18	XRN2	RBBP4	SEC16A	RPL9	RPN2
AIFM1	RPS4X	RUVBL1	RACK1	TARDBP	WWP2
HSD17B10	SAMM50	AGK	DNAJA2	TRIM28	ACTA2
MATR3	EFTUD2	HNRNPK	NOP56	STOML2	DERL1
DDX5	ATAD3B	PRKDC	DPM1	ERLIN1	SEC61B
SMARCC2	ABHD12	HNRNPUL1	RPS10	MSH2	PDK3
SMARCC1	SNRPF	ACOT9	HACD3	SSR1	MTX2
SMARCD1	WDR6	VDAC3	SMARCD2	ESYT2	RPS14
FASN	DNAJA3	VDAC1	RBM14	RBFOX2	DDX3X
PUF60	TECR	NTPCR	HNRNPF	RPL13	POMGNT2
RFC3	IMMT	CDS2	ICMT	DDX17	HNRNPL
ILF2	DPF2	ILF3	SLC25A4	RPL23	HNRNPU
ACTL6A	MYL6	ARID1B	MCM7	P4HA1	RPL38
CAND1	NOP58	RPL27	EMD	AKAP8L	RPS16
ACSL3	TMEM165	ATAD3A	SMARCA4	SLC25A10	RFC5
RPS23	TUBA1B	WWP1	TUBB6	EWSR1	LPCAT1
NUP93	RPL4	SEC61A1	CAD	COPB1	MYBBP1A
ALDH3A2	MCM3	PTBP1	PRPF8	CTNND1	SLC16A1
SLC25A1	RPS2	EEF1A1	TIMM23	NONO	SMARCE1
MSH6	SLC25A22	BCL7C	HNRNPM	AUP1	NCLN
SLC25A5	SNRPE	CCDC47	SLC25A11	SNRPD3	VDAC2
PELO	SLC25A13	DNAJB11	TMEM126A	TUBB4B	ERCC2
AFG3L2	TMTC3	FKBP8	TUBA1C	SLC25A12	LBR
CDK1	DDX39A	PARP1	BAG2	PCBP2	RPS27

Fig. 1

A

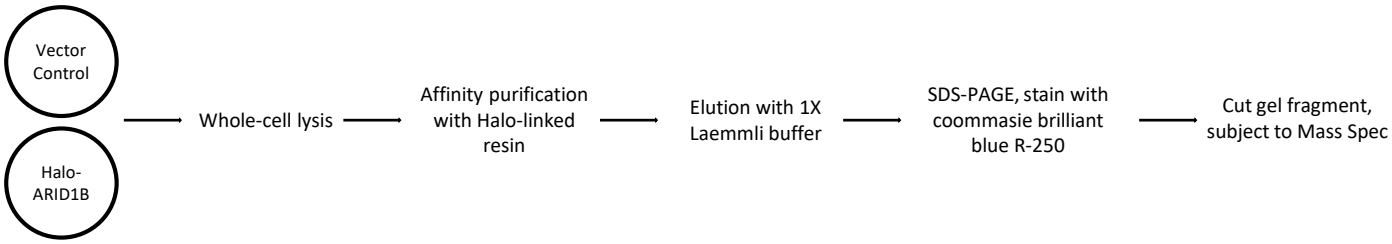
Vector Control
Halo-ARID1B
Whole-cell lysis
Affinity purification with Halo-linked resin
Elution with 1X Laemmli buffer
SDS-PAGE, stain with coommasie brilliant blue R-250
Cut gel fragment, subject to Mass Spec

B

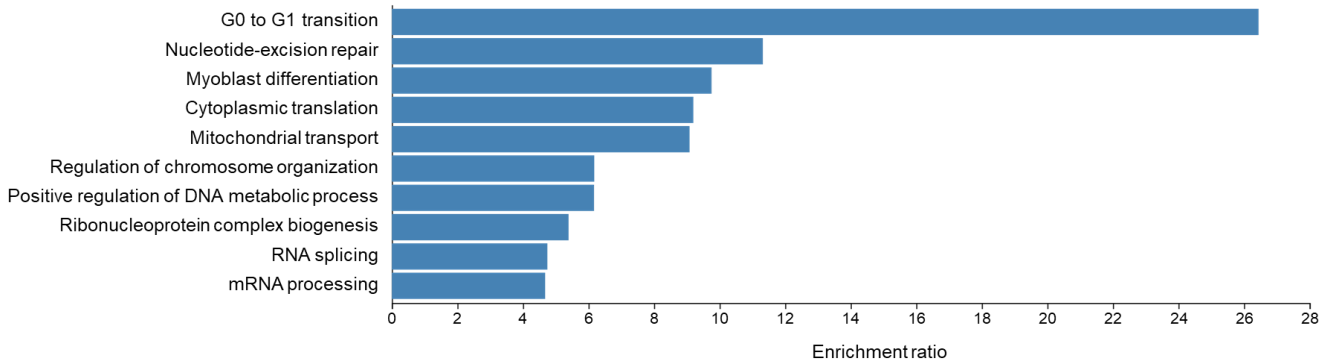
G0 to G1 transition
Nucleotide-excision repair
Myoblast differentiation
Cytoplasmic translation
Mitochondrial transport
Regulation of chromosome organization
Positive regulation of DNA metabolic process
Ribonucleoprotein complex biogenesis
RNA splicing
mRNA processing
0
2
4
6
8
10
12
14
16
18
20
22
24
26
28
Enrichment ratio

C

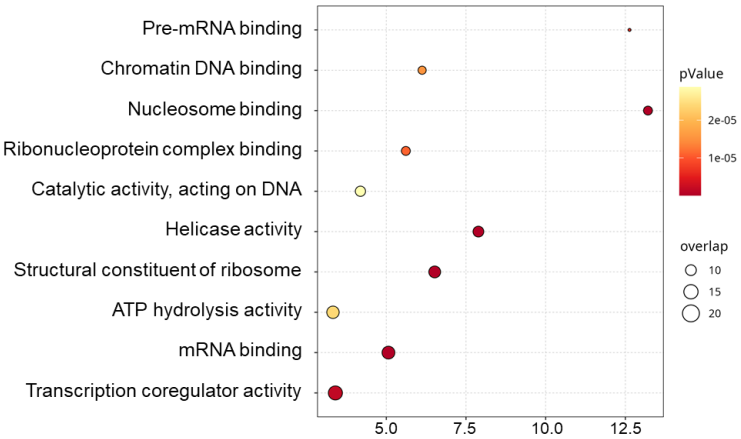
Pre-mRNA binding
Chromatin DNA binding
Nucleosome binding
Ribonucleoprotein complex binding
Catalytic activity, acting on DNA
Helicase activity
Structural constituent of ribosome
ATP hydrolysis activity
mRNA binding
Transcription coregulator activity
5.0
7.5
10.0
12.5
pValue
2e-05
1e-05
overlap
10
15
20

D

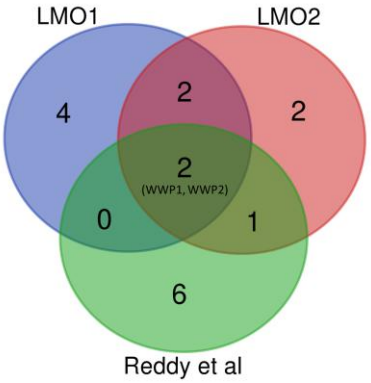
LMO1
LMO2
4
2
2
2
(WWP1, WWP2)
0
1
6
Reddy et al

Fig. 2

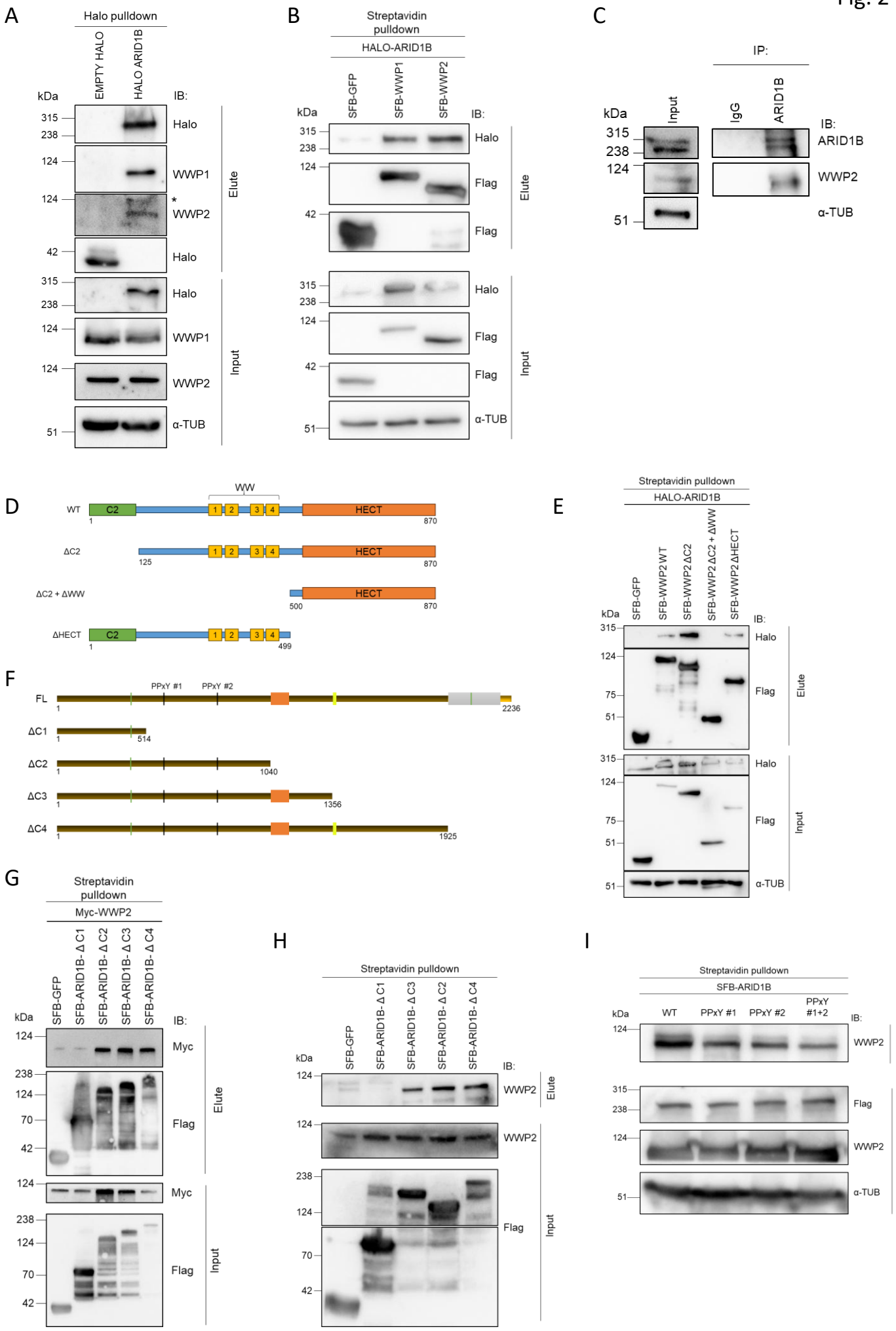
A
Halo pulldown
EMPTY HALO
HALO ARID1B
kDa
IB:
315
238
124
124
42
315
238
124
124
51
Halo
WWP1
WWP2
Halo
Halo
WWP1
WWP2
α-TUB
Elute
Input
B
Streptavidin pulldown
HALO-ARID1B
SFB-GFP
SFB-WWP1
SFB-WWP2
kDa
IB:
315
238
124
42
315
238
124
42
51
Halo
Flag
Flag
Halo
Flag
Flag
α-TUB
Elute
Input
C
IP:
Input
IgG
ARID1B
kDa
IB:
315
238
124
51
ARID1B
WWP2
α-TUB
D
WW
WT
C2
1
2
3
4
HECT
1
870
ΔC2
125
870
ΔC2 + ΔWW
500
870
ΔHECT
499
E
Streptavidin pulldown
HALO-ARID1B
SFB-GFP
SFB-WWP2 WT
SFB-WWP2 ΔC2
SFB-WWP2 ΔC2 + ΔWW
SFB-WWP2 ΔHECT
kDa
IB:
315
124
75
51
315
124
75
51
51
Halo
Flag
Halo
Flag
α-TUB
Elute
Input
F
PPxY #1
PPxY #2
FL
1
2236
ΔC1
1
514
ΔC2
1
1040
ΔC3
1
1356
ΔC4
1
1925
G
Streptavidin pulldown
Myc-WWP2
SFB-GFP
SFB-ARID1B- Δ C1
SFB-ARID1B- Δ C2
SFB-ARID1B- Δ C3
SFB-ARID1B- Δ C4
kDa
IB:
124
238
124
70
42
124
238
124
70
42
Myc
Flag
Myc
Flag
Elute
Input
H
Streptavidin pulldown
SFB-GFP
SFB-ARID1B- Δ C1
SFB-ARID1B- Δ C3
SFB-ARID1B- Δ C2
SFB-ARID1B- Δ C4
kDa
IB:
124
124
238
124
70
42
WWP2
WWP2
Flag
Elute
Input
I
Streptavidin pulldown
SFB-ARID1B
WT
PPxY #1
PPxY #2
PPxY #1+2
kDa
IB:
124
315
238
124
51
WWP2
Flag
WWP2
α-TUB
Elute
Input

Fig. 3

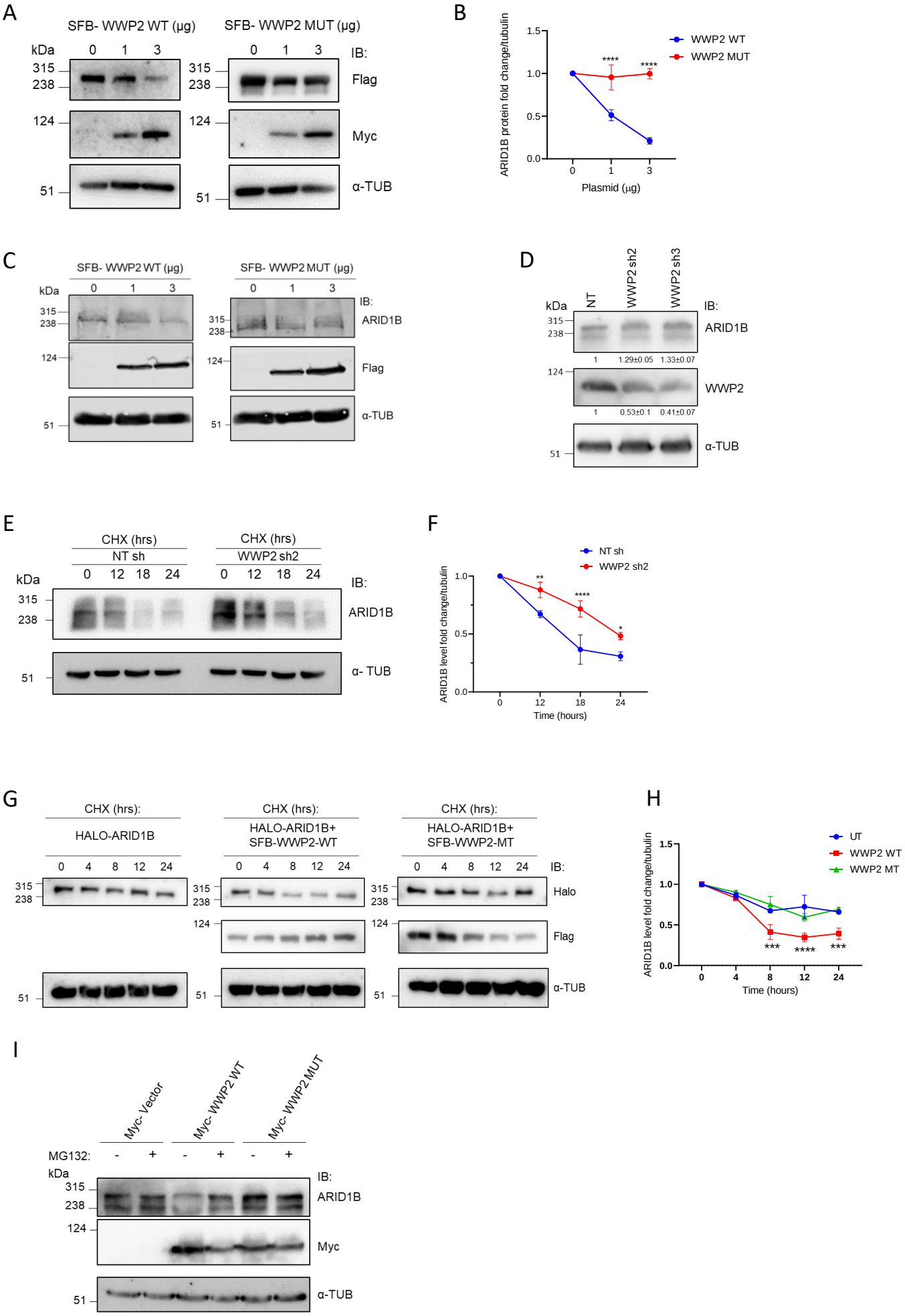
A
SFB- WWP2 WT (μg)
SFB- WWP2 MUT (μg)
kDa
0 1 3
IB:
315
238
124
51
Flag
Myc
α-TUB
B
ARID1B protein fold change/tubulin
Plasmid (μg)
WWP2 WT
WWP2 MUT
****
C
ARID1B
D
NT
WWP2 sh2
WWP2 sh3
1 1.29±0.05 1.33±0.07
1 0.53±0.1 0.41±0.07
WWP2
E
CHX (hrs)
NT sh
WWP2 sh2
0 12 18 24
α- TUB
F
ARID1B level fold change/tubulin
Time (hours)
NT sh
WWP2 sh2
**
*
G
CHX (hrs):
HALO-ARID1B
HALO-ARID1B+ SFB-WWP2-WT
HALO-ARID1B+ SFB-WWP2-MT
0 4 8 12 24
Halo
H
UT
WWP2 WT
WWP2 MT
***
I
Myc- Vector
Myc- WWP2 WT
Myc- WWP2 MUT
MG132:
-
+

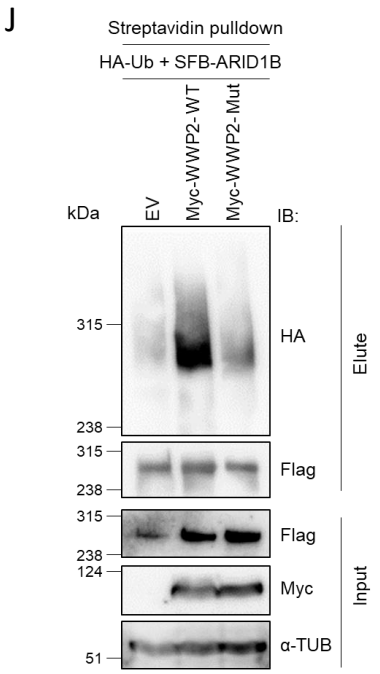
J
Streptavidin pulldown
HA-Ub + SFB-ARID1B
EV
Myc-WWP2-WT
Myc-WWP2-Mut
kDa
IB:
315
238
HA
Elute
315
238
Flag
315
238
Flag
124
Myc
Input
51
α-TUB

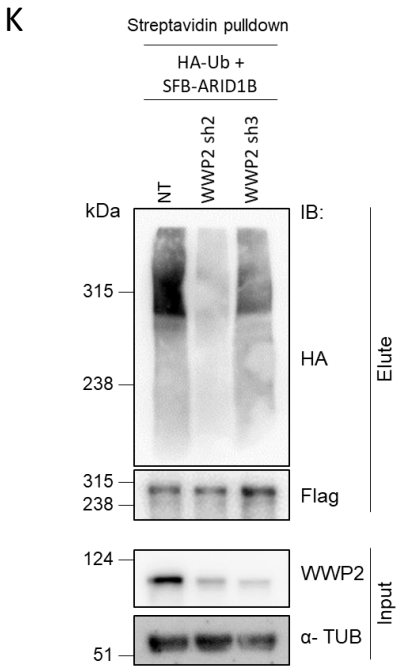
K
Streptavidin pulldown
HA-Ub +
SFB-ARID1B
NT
WWP2 sh2
WWP2 sh3
kDa
IB:
315
238
HA
Elute
315
238
Flag
124
WWP2
Input
51
α- TUB

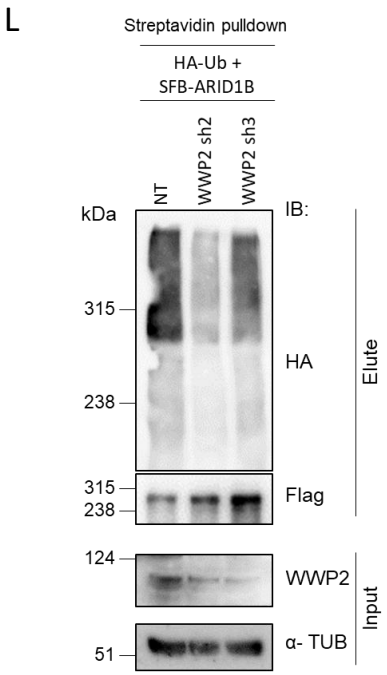
L
Streptavidin pulldown
HA-Ub +
SFB-ARID1B
NT
WWP2 sh2
WWP2 sh3
kDa
IB:
315
238
HA
Elute
315
238
Flag
124
WWP2
Input
51
α- TUB

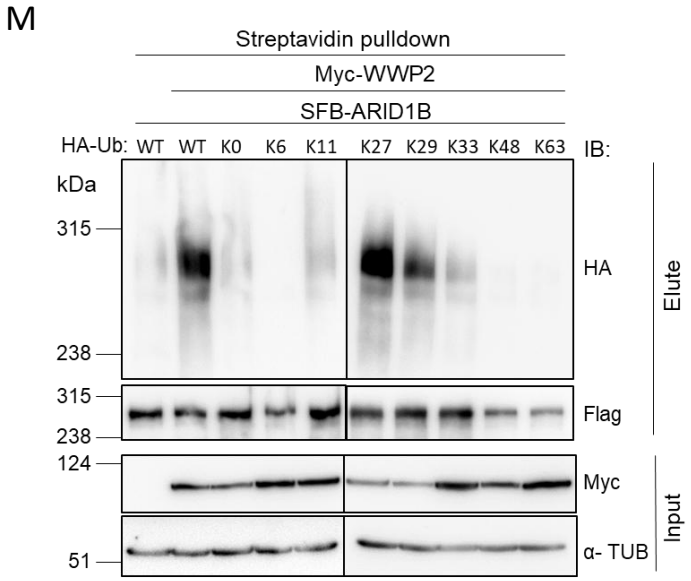
M
Streptavidin pulldown
Myc-WWP2
SFB-ARID1B
HA-Ub: WT WT K0 K6 K11 K27 K29 K33 K48 K63
IB:
kDa
315
238
HA
Elute
315
238
Flag
124
Myc
Input
51
α- TUB

Fig. 4

A

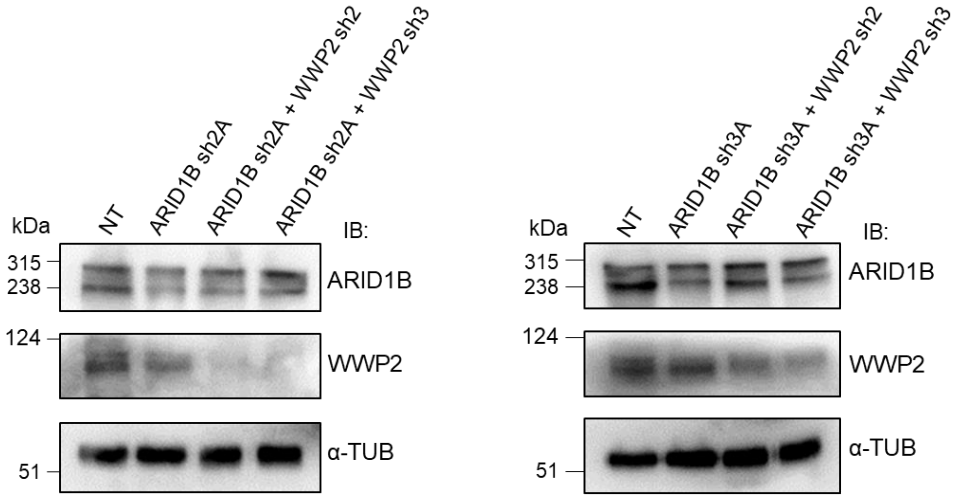

B

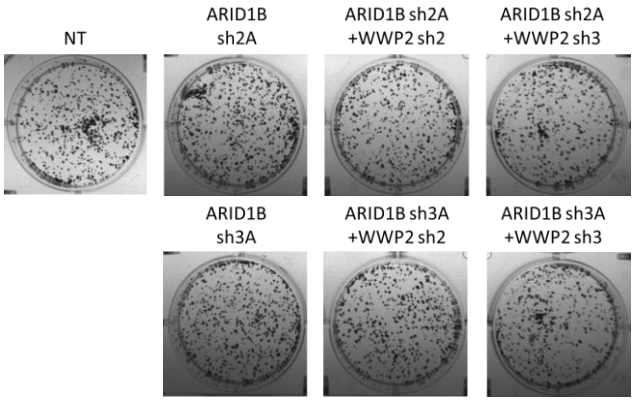

C

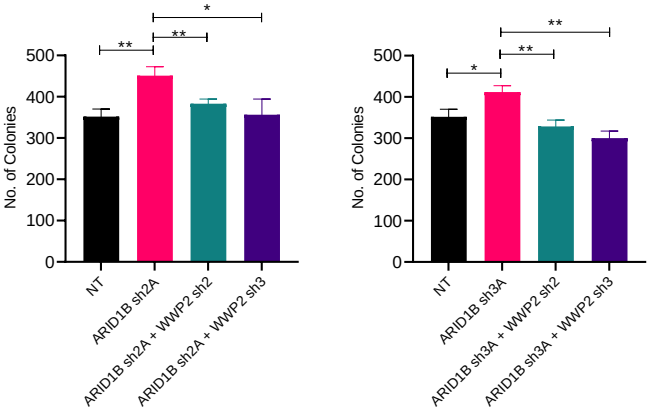

D

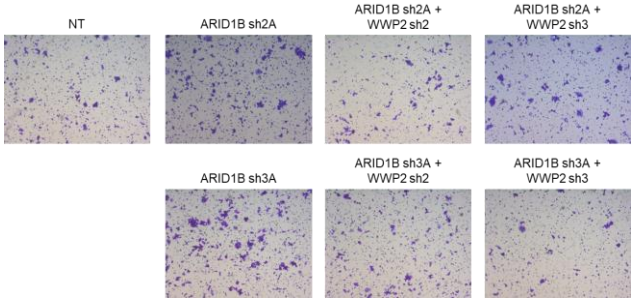

E

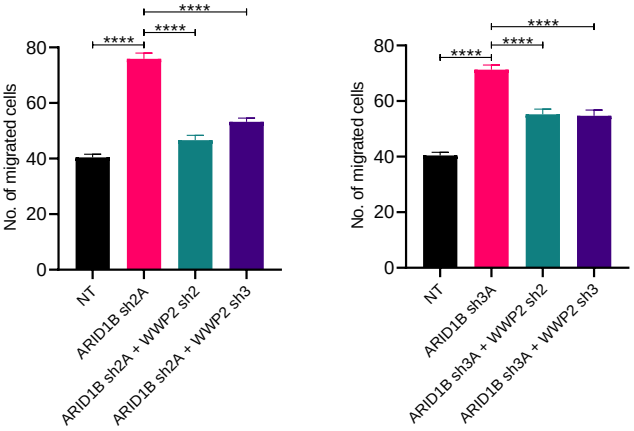

F

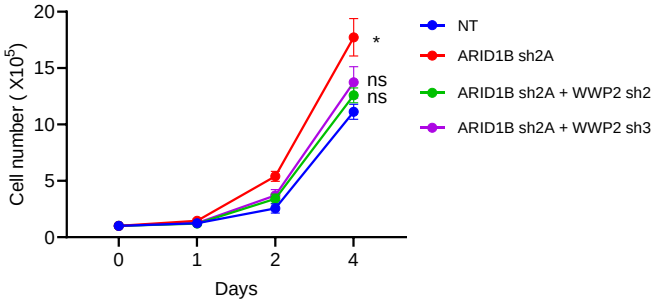

G

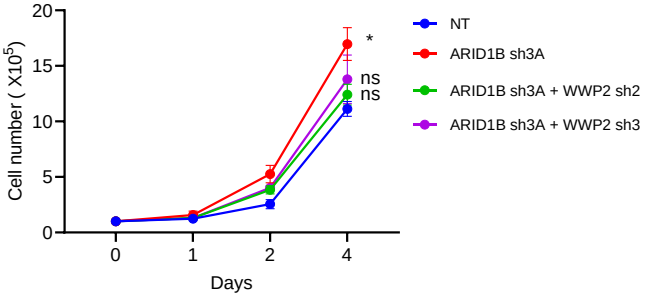

Fig 5: Graphical abstract

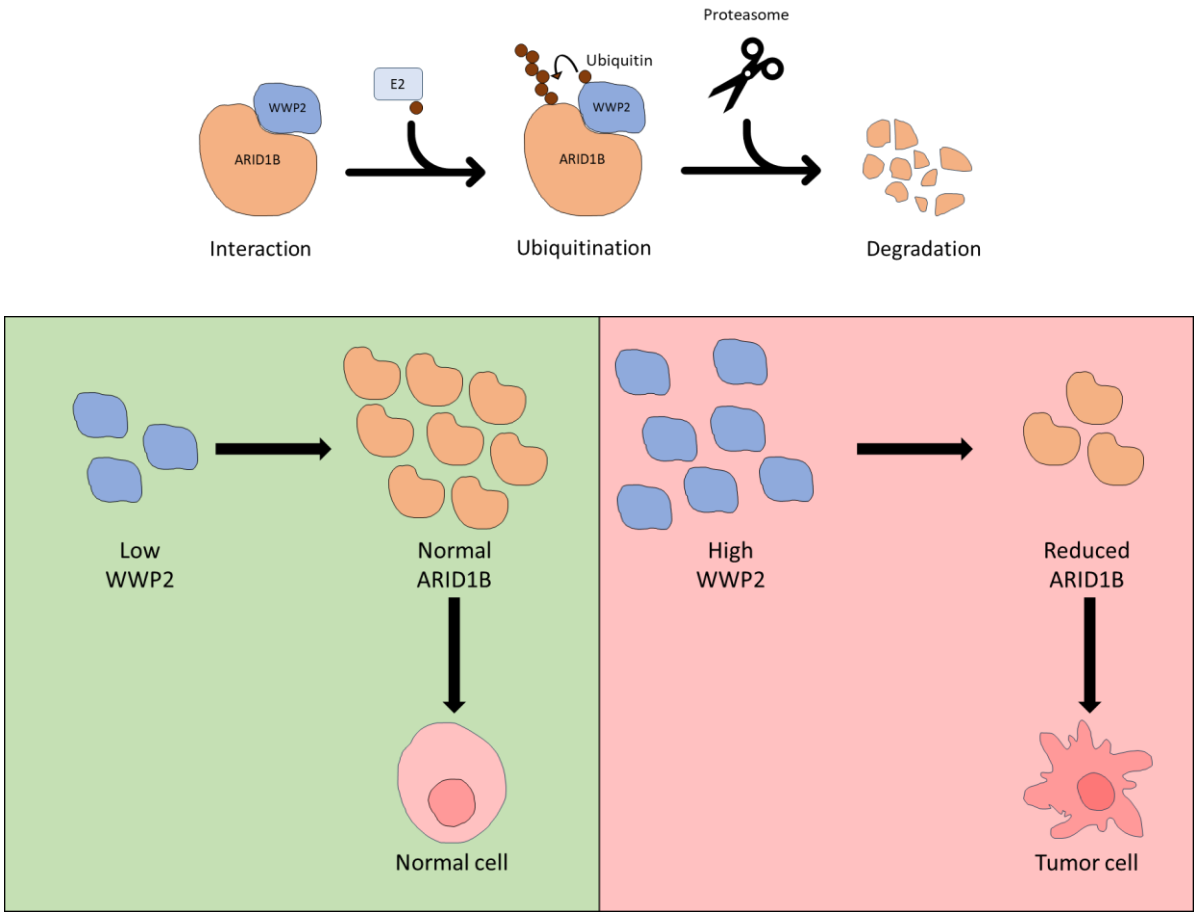

Supp. Fig. 1

A

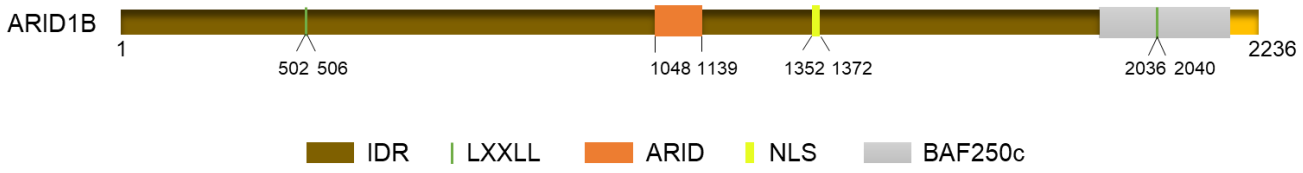
ARID1B
1
502 506
1048 1139
1352 1372
2036 2040
2236
IDR
LXXLL
ARID
NLS
BAF250c

B

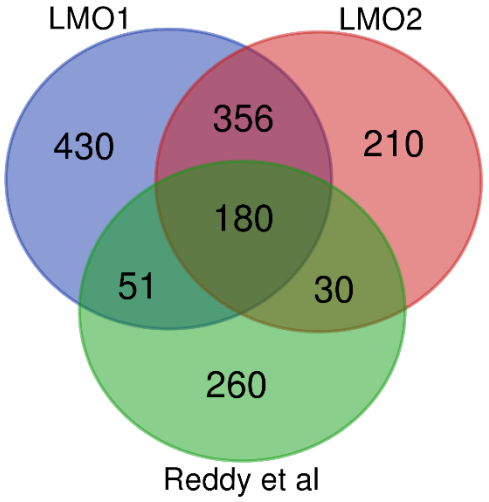
LMO1
LMO2
Reddy et al
430
356
210
180
51
30
260

Supp. Fig. 2

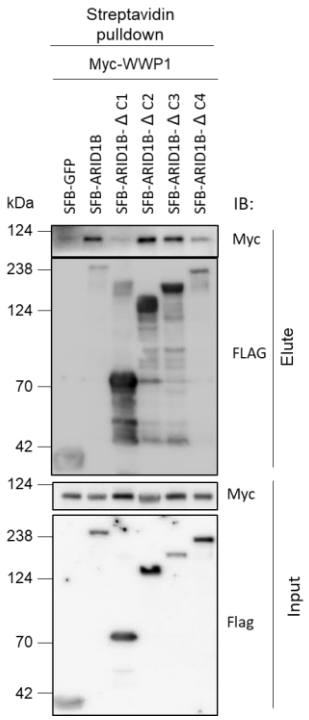
Streptavidin pulldown
Myc-WWP1
SFB-GFP
SFB-ARID1B
SFB-ARID1B- Δ C1
SFB-ARID1B- Δ C2
SFB-ARID1B- Δ C3
SFB-ARID1B- Δ C4
kDa
IB:
124
238
124
70
42
Myc
FLAG
Elute
124
Myc
238
124
70
42
Flag
Input

Supp. Fig. 3

A

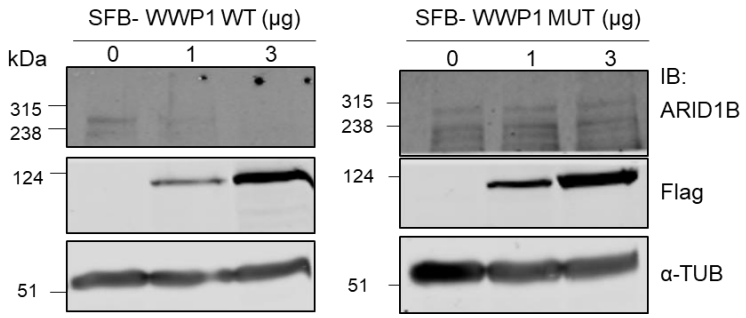

B

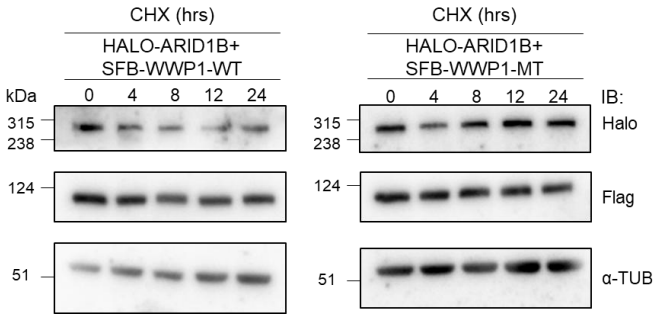

C

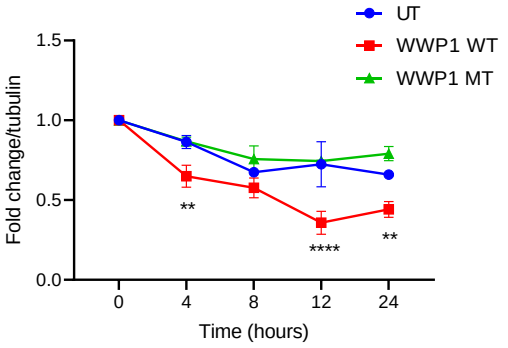

Supp. Fig. 4

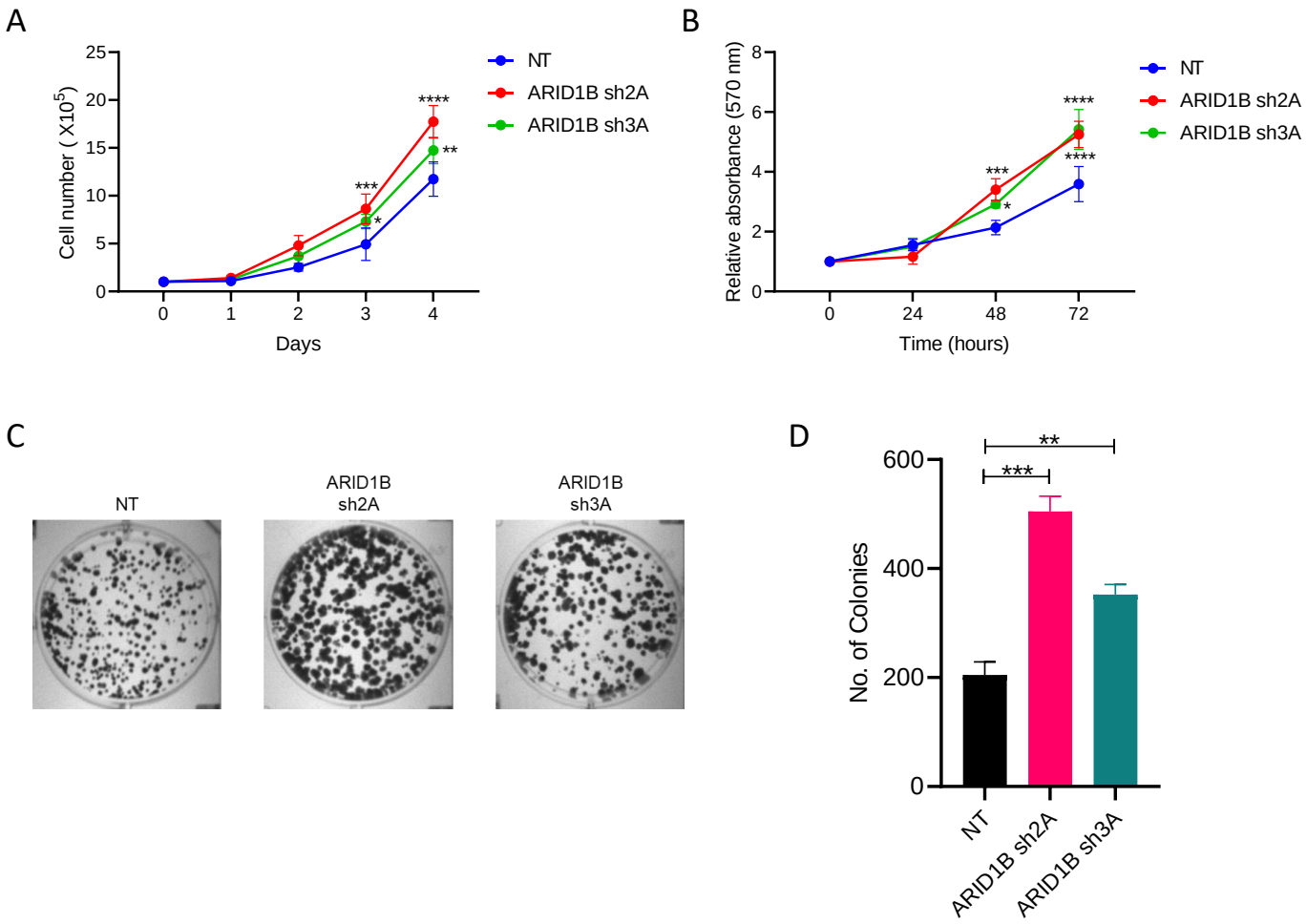
A
Cell number (X10^5)
Days
NT
ARID1B sh2A
ARID1B sh3A
B
Relative absorbance (570 nm)
Time (hours)
C
NT
ARID1B sh2A
ARID1B sh3A
D
No. of Colonies

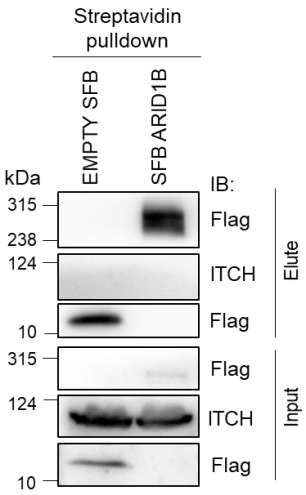
Streptavidin
pulldown
EMPTY SFB
SFB ARID1B
kDa
IB:
315
238
124
10
Flag
ITCH
Flag
Elute
315
124
10
Flag
ITCH
Flag
Input